

## Search for muonium-to-antimuonium conversion

G. M. Marshall,\* J. B. Warren, C. J. Oram, and R. F. Kiefl

*University of British Columbia, Vancouver, British Columbia, Canada V6T 2A6*

(Received 28 July 1981)

A new measurement is described which sets an upper limit on the coupling constant for conversion of muonium ( $\mu^+e^-$ ) to antimuonium ( $\mu^-e^+$ ) of  $42G_F$ , where  $G_F$  is the Fermi coupling constant. Muonium atoms were formed in layers of fine silica powder separated by vacuum drift regions. The presence of  $\mu^-$  was searched for using the signature of a Ca 2P-1S muonic x ray from calcium oxide layers adjacent to the drift regions. Results were also obtained with an Ar target.

## I. INTRODUCTION

The observation of rare processes which violate an established conservation law, such as that of muon number, may provide valuable clues concerning the correct structure of unified gauge theories. One such process is the conversion of the muonium ( $\mu^+e^-$ ) atom in the 1S state to antimuonium ( $\mu^-e^+$ ). However, interest in this conversion predates modern theories because of an ambiguity which existed in the form of muon-number conservation; the usual additive law forbids it while a less stringent multiplicative, parity-type scheme allows the conversion interaction.<sup>1</sup>

If lepton numbers are defined such that  $L_l = +1$  for  $l^-$  and  $\nu_l$ ,  $L_l = -1$  for  $l^+$  and  $\bar{\nu}_l$ , and zero for other particles, where  $l$  stands for  $e$ ,  $\mu$ , or  $\tau$ , the additive formulation demands  $\sum L_l$  constant for each  $l$ , and the unobserved reactions  $\mu \rightarrow e\gamma$ ,  $\mu \rightarrow 3e$ ,  $\mu(Z,A) \rightarrow e(Z,A)$ , and  $\nu_\mu(Z,A) \rightarrow e(Z',A)$  are not allowed. The multiplicative scheme, demanding  $\sum(L_e + L_\mu + L_\tau)$  and, for instance,<sup>2</sup>  $(-1)^{\sum(L_\mu + L_\tau)}$  or  $(-1)^{\sum(L_e + L_\tau)}$  constant likewise forbids them but, in contrast, permits interactions such as (1)  $\mu^+e^- \rightarrow \mu^-e^+$ , (2)  $e^-e^- \rightarrow \mu^-\mu^-$ , and (3)  $\mu^+ \rightarrow e^+\bar{\nu}_e\nu_\mu$ .

The four-fermion current-current Hamiltonian which might describe interactions (1) and (2) is<sup>1,3</sup>

$$H = (G/\sqrt{2})\bar{\psi}_\mu\gamma_\lambda(1-\gamma^5)\psi_e\bar{\psi}_\mu\gamma^\lambda(1-\gamma^5)\psi_e + \text{H.c.}, \quad (1.1)$$

in which the  $V-A$  neutral current couples muon and electron fields. An upper limit for the value of  $G$  of  $5800G_F$ , where  $G_F$  is the Fermi coupling constant, was established by a search for muonium

conversion to antimuonium in argon gas.<sup>4</sup> A later experiment improved this to  $610G_F$  by searching for the reaction  $e^-e^- \rightarrow \mu^-\mu^-$  in colliding beams of electrons.<sup>5</sup> These constitute the best previous direct measurements of the limit for  $G$ . A more recent investigation of the ambiguity in muon-number conservation searched for "wrong" neutrinos ( $\bar{\nu}_e + \nu_\mu$ ) from positive-muon decay [reaction (3)] and was able to show good agreement with the additive scheme.<sup>6</sup> However, no information on the value of  $G$  can be inferred from the results without recourse to specific models,<sup>2</sup> since muon decay is a charged-current interaction. The purpose of this experiment is to reduce further the upper limit on  $G$  via a direct search for muonium conversion to antimuonium, by taking advantage of technical developments in low-energy muon beams, high-resolution muonic-x-ray detection, and a target capable of creating muonium atoms in a vacuum environment where conversion to antimuonium is not highly suppressed.

## II. EXPERIMENTAL METHOD

## A. Muonium in vacuum

A nonzero value for the coupling constant  $G$  implies that the eigenstates of the full Hamiltonian are linear combinations of muonium and antimuonium states, leading to the possibility of conversion. In the presence of an electromagnetic interaction, the sign of which is opposite for muonium and antimuonium, conversion is suppressed by a factor depending on its strength relative to the weak interaction.<sup>3</sup> If the electromagnetic interac-

tion is much stronger, the eigenstates approach pure muonium and pure antimuonium, and conversion is thereby inhibited. A uniform magnetic field of 25 mG is sufficient to halve the conversion in vacuum of the hyperfine states  $(F, m_f) = (1, \pm 1)$  of  $1S$  muonium, while interaction with matter vastly reduces the conversion probability for all states. Therein lies the reason that more sensitive muonium-antimuonium searches have not yet been performed; muonium is easily produced by stopping muons in an appropriate medium, but the medium is generally not conducive to conversion.

A possible solution is to produce muonium in an inhomogeneous target such that, after formation in a suitable material, it may move into a region of field-free vacuum. This was first attempted using a hot metal foil for muonium production.<sup>7</sup> More recent experiments using a stack of thin gold foils initially promising<sup>8</sup> but the results could not be reproduced.<sup>9</sup> In the present work a slightly different target configuration is used which employs the foil geometry but depends on the ease with which muons in fine silica powder will form muonium in the powder interstices.

It has been previously shown<sup>10</sup> that muons coming to rest in a target of silica powder particles (radii of  $3.5 \times 10^{-9}$  m and  $7.0 \times 10^{-9}$  m) form muonium which can react via spin exchange with oxygen molecules introduced into the voids between particles. The bimolecular rate constant for the reaction is proportional to the spin exchange cross section times the mean relative collision velocity and is consistent with the same quantity measured with argon and nitrogen gas moderators<sup>11</sup> at room temperature. In the gas phase moderators the mean thermal speed for muonium ( $7400$  m sec<sup>-1</sup> at room temperature) is 17 times that of oxygen, so the equality of rate constants strongly indicates that muonium in the voids of the powder target is moving thermally rather than binding or being trapped at the particle surfaces. In an evacuated target of silica particles (Cab-O-Sil EH5, made by Cabot Corporation, Boston; mean radius  $3.5 \times 10^{-9}$  m, density  $0.032$  g cm<sup>-3</sup>), muonium then has a mean free path of about  $3 \times 10^{-7}$  m, or a mean time between collisions of only  $4 \times 10^{-11}$  sec. Because of the collision interaction, muonium conversion under these conditions is still seriously suppressed. However, a muonium atom can migrate within the voids for distances of the order of a tenth of a millimeter before decay. In particular, muonium formed near the surface of an evacuated layer of powder may leave the layer prior to decay.

To take advantage of this a target was assembled consisting of 17 layers of silica powder, separated by drift regions of 4.1 mm on average (see Fig. 1). Each powder layer was approximately 0.3 mm ( $0.85$  mg cm<sup>-2</sup>) thick, supported by a  $0.11$  mg cm<sup>-2</sup> elliptical collodion film, 20 cm by 10 cm, mounted on an expanded polystyrene frame. The layers were set at an angle  $30^\circ$  from the horizontal so as to present a circular profile in the beam direction. This was done in order to allow the powder to rest on the slanted collodion surface which had been slightly roughened by attaching some powder particles ( $0.04$  mg cm<sup>-2</sup> average) to it with an acetone-water spray. It also served to double the thickness of material per layer along the beam direction so that more muons could be stopped in one layer. The lower side of the collodion film was coated by evaporation with calcium metal which was then allowed to oxidize in a dry atmosphere. The resulting CaO surface, about  $5 \times 10^{-3}$  mg cm<sup>-2</sup>, would capture the negative muons from antimuonium atoms arising from conversion of muonium escaping the adjacent silica layer and traversing the drift region (where conversion would not be inhibited by collisions). The sig-

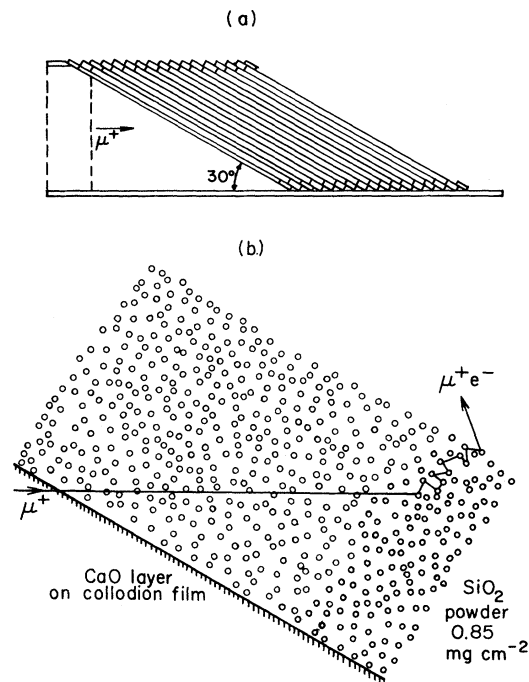


FIG. 1. Side view of the layered silica-powder target: (a) stack of 17 films supporting the powder, (b) an enlarged portion of one layer, showing formation of muonium in the drift region from a thermalizing muon beam.

nature denoting a conversion event is the calcium muonic  $2P-1S$  x ray at 784 keV.

### B. The muon beam

The data reported here were taken using the M13 low-energy pion and muon beam line<sup>12</sup> at TRIUMF. A beam of 29-MeV/c positive surface muons<sup>13</sup> from pion decay at the surface of the graphite production target was ranged to stop in the stack of silica-powder layers after passing through a thin scintillation counter (MU). For a primary 500-MeV proton current of  $25 \mu A$  striking a 1-cm-long graphite production target, a flux of over  $2.5 \times 10^5$  muons could be obtained in an area of  $2 \times 5 \text{ cm}^2$ , but the acceptance aperture of the channel was limited in order to reduce particles (especially positrons) at the edges of the beam spot. The incident muon rate at the MU counter was typically  $1.7 \times 10^5 \text{ sec}^{-1}$ . The range spread of the beam, measured from an integral range curve, was  $25 \text{ mg cm}^{-2}$ , reasonably well matched to the effective layered silica target thickness of  $30 \text{ mg cm}^{-2}$ . The positron contamination of the beam was approximately equal to the muon flux and was minimized by making the graphite production target small (reducing conversion of gammas from  $\pi^0$  decays) and carefully steering the proton beam to the edge nearest the M13 aperture.<sup>12</sup>

In order to reduce the introduction of possible systematic uncertainties, calibrate the detection sys-

tem, and facilitate the analysis of the data, the beam line was also run in the negative-particle mode at 29 MeV/c. Although the strong absorption of stopped negative pions in the production target destroys the possibility of a negative surface muon beam, a flux of  $\mu^-$  at this momentum of about 1.0% of the surface  $\mu^+$  flux does exist from  $\pi^-$  decays in the target region. Little difference in beam profile between  $\mu^+$  and  $\mu^-$  was observed. Furthermore, the charge of the beam will not significantly affect the range spread because the energy loss processes occurring above about 100 keV, which substantially determine the range of 4-MeV surface muons, are charge independent. The  $\mu^-$  data were thus useful in establishing the fraction of muons stopping in the active silica component of the target times the efficiency (solid angle and photopeak) for detection of silicon  $2P-1S$  muonic x rays at 400 keV. Correcting this product for relative capture ratios, attenuation factors, and photopeak efficiencies for calcium muonic x rays then provided a measurement important for the determination of the sensitivity of the conversion experiment.

### C. Detection system and background suppression

A schematic diagram of the apparatus in the conversion target region is shown in Fig. 2. The target was enclosed in a vacuum pipe attached to

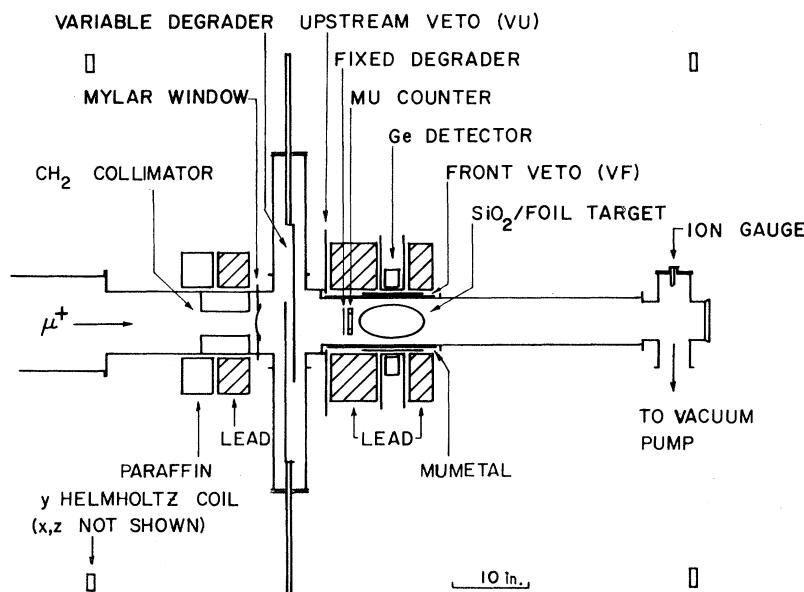


FIG. 2. Plan view of the target region.

the end of the beam line and separated from it by a 0.12-mm Mylar vacuum window. After penetrating the window, the muon beam was degraded and detected by 0.25-mm thin scintillator (MU) of 5-cm diameter which could discriminate muons from beam positrons by pulse height. Most of the beam positrons passed harmlessly through the target into the region downstream.

A thin mumetal shield sheathed the 3-mm-thick Al pipe surrounding the target. The entire apparatus was contained within a set of three mutually perpendicular 200-cm-square Helmholtz-coil pairs automatically controlled by a triaxial saturable inductor magnetometer probe close to the target position. The coils alone could maintain a magnetic field of less than 20 mG over the target region; the coil performance was actually much better but the gradient of the ambient field was a limiting factor. The mumetal was included to eliminate the field gradient and allow the maintenance of a field of less than 4 mG over the target region for the duration of the experiment.

Two large, high-efficiency, high-resolution germanium detectors viewed the conversion target from either side for the detection of possible muonic x rays. One was a 71.5-cm<sup>3</sup> intrinsic detector, while the other was a 103.2-cm<sup>3</sup> lithium-drifted device. Both achieved a resolution of better than 1.9 keV (full width at half maximum) at 1.33 MeV under beam conditions. A large scintillation counter (VF) covered the face of each detector for identification of events due to charged particles (mostly muon-decay positrons). Other counters (VU) were placed upstream to veto events from beam positrons surviving a polyethylene (CH<sub>2</sub>) collimator at the end of the beam tube.

Substantial quantities of lead and paraffin, not all of which are shown in Fig. 2, were used to shield the germanium detectors from background radiation in the form of  $\gamma$ 's and neutrons. Several very-low-intensity lines attributable<sup>14</sup> to neutron interactions were visible in the final data set.

Pulse-height event acquisition via a pulse-height analyzer (PHA) was enabled by a gate initiated by an incident muon. However, the beam intensity was such that at least one muon was in the target for a large fraction of the time. In addition, the following occurrences would suppress storage of an event: (1) PHA busy, (2) pulse pile-up in the Ge crystal in which the event was detected, (3) a fast coincidence between the Ge signal and any charged-particle veto scintillator (VF or VU), and (4) a nonquiescent level of the Ge amplifier output

present when the event was detected. The last criterion was imposed because of the occasionally very large amount of energy deposited in each Ge detector, especially by muon-decay positrons (estimated at  $10^5$  MeV sec<sup>-1</sup>), which could cause saturation of the resolution-optimized charge-sensitive preamplifiers. The dead time introduced by the four sources of event rejection was monitored continuously as the data were acquired.

### III. ANALYSIS

The determination of an upper limit for the conversion of muonium to antimuonium from this experiment requires a knowledge of the behavior of a muon entering the layered-silica-target region. The number of muonic-x-ray events ( $N_0$ ) observed in a calcium 2P-1S photopeak at 784 keV can be related to the number ( $N$ ) of muons incident during the Ge detector live time by the expression  $N_0 = PN$ , where  $P$  is given by the product

$$P = F(\text{Si})F(\text{Mu})F(\text{vac})F(\text{drift})P(\text{conv})\epsilon \quad (3.1)$$

and the factors are defined as follows:

$F(\text{Si})$  = fraction of incident muons stopping in the silica layers.

$F(\text{Mu})$  = muonium-formation fraction in silica powder.

$F(\text{vac})$  = fraction of muonium formed in evacuated silica powder which emerges into the voids between particles before decaying.

$F(\text{drift})$  = fraction of muonium in the voids of a silica-powder layer which migrates before decay to the drift region separating the layers.

$P(\text{conv})$  = the probability, in terms of the coupling constant  $G$ , that muonium traversing the field-free drift region will reach the CaO surface on the opposite side as antimuonium.

$\epsilon$  = the overall efficiency for detecting a calcium 2P-1S muonic x ray, including the relative capture ratio for Ca in CaO, the  $K_\alpha$  yield, attenuation factors, solid-angle acceptance, and photopeak efficiency.

The product  $F(\text{Si})\epsilon$  is obtained experimentally for each detector from negative muon beam data (Fig. 3). The probability, given an incident negative muon, of observing a silicon muonic 2P-1S x ray is the product of  $F(\text{Si})$ , the Si  $K_\alpha$  to total K x-ray intensity from silicon and oxygen in SiO<sub>2</sub> powder, and the efficiency (including solid angle, photopeak

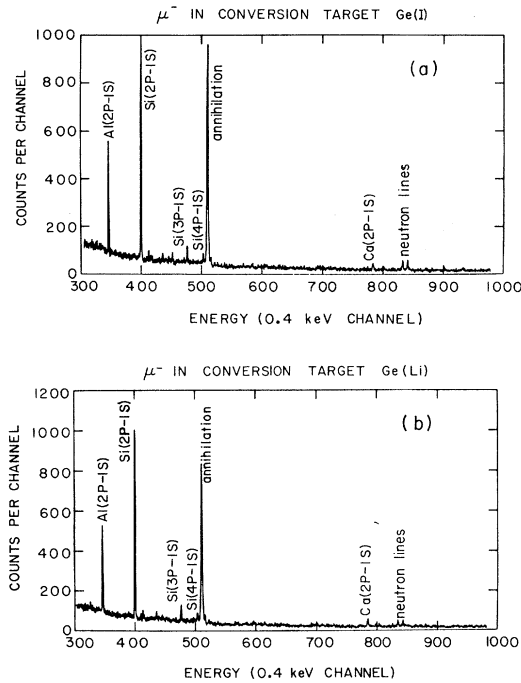


FIG. 3. Muonic-x-ray spectra from layered target, using 29-MeV/c  $\mu^-$ : (a) intrinsic Ge detector, (b) lithium-drifted Ge detector.

efficiency, and attenuation) of detection. The x-ray intensity ratios of  $\text{SiO}_2$  and CaO were measured from separate targets with the same apparatus, yielding a correction factor for Ca  $K_\alpha$  to the total  $K$  x-ray intensity from calcium oxide. After further corrections for relative photopeak efficiency and attenuation, the results were

$$\begin{aligned} F(\text{Si})\epsilon &= (1.80 \pm 0.26) \times 10^{-4}, & \text{Ge(I)} \\ F(\text{Si})\epsilon &= (2.30 \pm 0.35) \times 10^{-4}, & \text{Ge(Li)}. \end{aligned} \quad (3.2)$$

$F(\text{Mu})$ , the muonium-formation probability in silica powder, is measured by muonium-spin-rotation (MSR) techniques to be  $0.61 \pm 0.03$ .<sup>15</sup> The exponential relaxation of the muonium precession signal observed after the introduction of oxygen into the voids implies that the fraction of muonium reaching the voids before decay,  $F(\text{vac})$ , is about 0.97 (Ref. 10); a more sophisticated analysis of MSR data, assuming a diffusion mechanism within the spherical silica particles, yields a diffusion parameter<sup>10</sup> which in turn predicts<sup>16</sup> the fraction  $F(\text{vac})$  to be  $0.93 \pm 0.01$  for the grain radius of  $3.5 \times 10^{-9}$  m. The latter more pessimistic value is used to estimate the lower limit of  $P$ .

Once a muonium atom escapes the silica particles and moves through the voids, its location can

be described in a probabilistic sense by random walk techniques<sup>17</sup> via an effective motion parameter  $D = vs/3$ , where  $v$  is the mean speed and  $s$  the mean free path of muonium between collisions with silica spheres. The latter quantity is calculable from the silica particle radius and number density, so that  $D \sim 7.9 \text{ cm}^2 \text{ sec}^{-1}$ . For an ensemble of muonium atoms initially distributed uniformly in a homogeneous layer of thickness  $d$ , the probability  $q$  of escaping from one surface of the layer prior to decay is given by

$$q = (1 - e^{-\beta}) / 2\beta, \quad (3.3)$$

where  $\beta = (\lambda d^2 / D)^{1/2}$ , and  $\lambda$  is the muon decay rate. For the average powder layer thickness  $d = 0.27$  mm, the probability is 0.078. However, the layers were not exactly uniform; visually the coverage was estimated to be greater than  $\frac{2}{3}$ . The  $d^{-1}$  of dependence  $q$ , for  $d \gg (D/\lambda)^{1/2}$ , then allows the establishment of the limit

$$F(\text{drift}) > 0.052 \quad (3.4)$$

for the fraction of muonium atoms in vacuum which reach the drift space between layers before decay.

A search was made for evidence of muonium atoms decaying in vacuum at a distance of 1 cm from the surface of one silica-powder layer. A scintillator telescope of very narrow angular acceptance was aimed at the decay region, and used to provide a stop signal for a clock started by a muon incident on the layer. If muonium drifts with thermal velocity from the surface, an enhancement in the resulting muon-decay spectrum should occur at about  $2 \mu\text{sec}$  due to muonium drifting through the region viewed by the telescope. While such an effect was observed, giving

$$F(\text{drift}) = 0.095 \pm 0.050, \quad (3.5)$$

the result was not confirmed with different experimental arrangements, and hence this value is not used in the analysis of the data. It is, however, consistent with the result of Eq. (3.4). The major problem with these measurements is the high background from muons decaying in the silica layer and beam pipe.

The probability  $P(\text{conv})$  that a muonium atom will survive traversal of the 4.1-mm drift space and interact with the adjacent CaO surface as antimuonium depends on the quantity  $(G/G_F)^2$ , and can be calculated by assuming a thermal distribution of speed and a uniform angular emittance from the

silica surface. The value obtained is

$$P(\text{conv}) = 2.5 \times 10^{-6} (G/G_F)^2. \quad (3.6)$$

Because of the large cross section for inelastic scattering of  $\mu^-e^+$ , leading to the formation of muonic atoms, any antimuonium reaching the CaO surface will result in a  $K$  x-ray from either calcium or oxygen.

Lower limits for the right-hand side of Eq. (3.1) can be calculated simply by inserting the quoted values. The results are

$$P > (1.33 \pm 0.20) \times 10^{-11} (G/G_F)^2, \quad \text{Ge(I)}, \quad (3.7)$$

$$P > (1.70 \pm 0.27) \times 10^{-11} (G/G_F)^2, \quad \text{Ge(Li)}.$$

The total number of positive muons entering the target during the experiment was  $2.32 \times 10^{10}$ . Allowing for live times of the two detectors (82 and 92%, respectively), two values of  $N$  can be derived and multiplied by the appropriate value of  $P$ . Combining the two results gives the summed experimental sensitivity

$$PN > (0.61 \pm 0.09) (G/G_F)^2. \quad (3.8)$$

This number is to be compared with the Ca 2P-1S muonic-x-ray intensity observed in the Ge pulse-height spectra, shown for the energy range 740–850 keV (Fig. 4). There is no evidence of any photopeak at 784 keV in either case. Both show a background  $^{54}\text{Mn}$  line at 835 keV, from iron in the shielding, which was used for calibration and off-line gain corrections. There is evidence of a low-intensity peak at 804 keV, especially in the more efficient Ge(Li) detector, which may result from inelastic scattering of neutrons by the detector material (the peak shows a hint of the high-energy broadening characteristic of neutron-induced lines). Neutron irradiation of Ge crystals shows a rich structure, not all of which can be attributed to known  $\gamma$  rays.<sup>14</sup>

The spectra of Fig. 4 were analyzed with a multiparameter  $\chi^2$  minimization routine to determine the upper limits on the intensity of a possible photopeak at 784 keV. An estimate for linear background terms was made from data in the 740-to-800-keV region. After fixing the expected position and widths (1.62 and 1.68 keV, respectively, for the two spectra) for the Ca line, the analysis allowed variation of the peak intensity as well as the linear background terms, to fit a 15-keV region centered on the peak position. Details of this and other aspects of the experiment can be found elsewhere.<sup>18</sup> The values obtained were  $-153$  and  $-44$  counts,

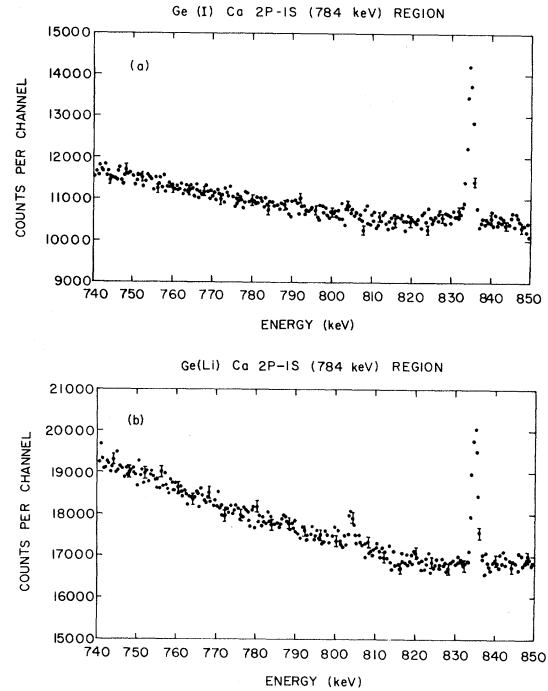


FIG. 4. Spectra from  $2.32 \times 10^{10} \mu^+$  incident on the layered target (see text). Note suppression of the zero on the vertical axes. (a) intrinsic Ge detector, (b) lithium-drifted Ge detector.

respectively, for the photopeak intensities, with positive standard deviations of 277 and 371. The one-standard-deviation limit on the sum of the intensities is thus 463 counts.

#### IV. RESULTS

A comparison of the upper limit on the combined photopeak intensity ( $N_0$ ) with lower limit for the experimental sensitivity ( $PN$ ), a function of the coupling constant, yields directly a limit for  $G$ . At the 95% confidence level, the comparison allows  $G < 39G_F$ ; including the uncertainty in the limit for  $PN$ , Eq. (3.8), the final result is

$$G < 42G_F \quad (95\% \text{ C.L.}) \quad (4.1)$$

The limit can also be expressed in terms of the branching ratio  $R$  for the muon, in a system initially created as muonium and evolving in a field-free vacuum, to decay as  $\mu^-$  rather than  $\mu^+$ . If  $\delta$  is twice the matrix element of the conversion Hamiltonian  $H$  of Eq. (1.1), its value is  $2.1 \times 10^{-12} (G/G_F)eV$ . In terms of  $\delta$  and the muon decay rate,  $\lambda = 3.0 \times 10^{-10} eV$ , the branching ratio is<sup>3</sup>

$$R = \delta^2 / 2(\delta^2 + \lambda^2) . \quad (4.2)$$

The present experiment gives  $R < 0.04$ , compared with  $R < 0.50$  from a previous search for conversion<sup>3</sup> and  $R < 0.47$  from a search for electron-electron colliding beam production of muons.<sup>4</sup>

A high-purity argon gas target at room temperature and one atmosphere pressure, similar to that used by Amato *et al.*,<sup>3</sup> was also employed during the initial set-up of the apparatus and detection system. Using numbers quoted in that reference, corrected for more recent and precise measurements of the muonium formation fraction in argon ( $0.63 \pm 0.07$ , rather than unity),<sup>19</sup> an analysis of our argon data leads to the limit

$$G < 190G_F \text{ (95\% C.L.)} , \quad (4.3)$$

or  $R < 0.32$ . This value corresponds to a total of  $3.4 \times 10^9$  incident positive muons. The limit is set by the maximum number of argon muonic  $2P\text{-}1S$  x rays in the energy spectrum, which was determined

to be 1066 at the 95% confidence level. The x-ray detection probability for this target was also estimated using a negative muon beam at 29 MeV/c which allowed simple observation and measurement of both  $K_\alpha$  and  $K_\beta$  muonic x rays.

It does not at present seem possible to improve significantly the limit for  $G$  with the technique described here; the two limiting factors are the  $\gamma$  background, from bremsstrahlung from  $\mu^+$  decay positrons, and the low value of  $P$ .

#### ACKNOWLEDGMENTS

We would like to thank Mr. G. S. Clark, Mr. A. Morgan, and Mr. C. Stevens for capable assistance in the construction of the experimental components, and the operating staff of TRIUMF for providing excellent service. This work was supported by the Natural Sciences and Engineering Research Council of Canada and by the National Research Council.

\*Present address: Rutherford and Appleton Laboratories, Chilton, Didcot, Oxon OX11 0QX, England.

<sup>1</sup>G. Feinberg and S. Weinberg, *Phys. Rev. Lett.* **6**, 381 (1961). The first suggestion that conversion might be possible was made by B. Pontecorvo, *Zh. Eksp. Teor. Fiz.* **33**, 549 (1957) [*Sov. Phys.—JETP* **33**, 429 (1958)].

<sup>2</sup>The multiplicative law extended to the  $\tau$  generation is a feature of the model of E. Derman, *Phys. Rev. D* **19**, 317 (1979).

<sup>3</sup>G. Feinberg and S. Weinberg, *Phys. Rev.* **123**, 1439 (1961).

<sup>4</sup>J. J. Amato, P. Crane, V. W. Hughes, J. E. Rothberg, and P. A. Thompson, *Phys. Rev. Lett.* **21**, 1709 (1968).

<sup>5</sup>W. C. Barber, B. Gittelmann, D. C. Cheng, and G. K. O'Neill, *Phys. Rev. Lett.* **22**, 902 (1969).

<sup>6</sup>S. E. Willis, V. W. Hughes, P. Nemethy, R. L. Burman, D. R. F. Cochran, J. S. Frank, R. P. Redwine, J. Duclos, H. Kaspar, C. K. Hargrove, and U. Moser, *Phys. Rev. Lett.* **44**, 522 (1980); **45**, 1370 (*E*) (1980).

<sup>7</sup>K. R. Kendall, Ph.D. thesis, University of Arizona, 1972 (unpublished).

<sup>8</sup>B. A. Barnett, C. Y. Chang, P. Steinberg, G. B. Yodh, H. D. Orr, J. B. Carroll, M. Eckhause, J. R. Kane, C. P. Spence, and C. S. Hsieh, *Phys. Rev. A* **15**, 2246 (1977).

<sup>9</sup>W. Beer, P. R. Bolton, P. O. Egan, V. W. Hughes, D. C. Lu, F. G. Mariam, P. A. Souder, J. Vetter, M. Gladisch, G. zu Putlitz, U. Moser, L. J. Teig, R. S. Holmes, P. H. Steinberg, J. R. Kane, and R. Hartmann, in *Proceedings of the Eighth International*

*Conference on High Energy Physics and Nuclear Structure, Vancouver, Canada, 1979*, edited by D. F. Measday and A. W. Thomas (North-Holland, Amsterdam, 1980).

<sup>10</sup>G. M. Marshall, J. B. Warren, D. M. Garner, G. S. Clark, J. H. Brewer, and D. G. Fleming, *Phys. Lett.* **65A**, 351 (1978).

<sup>11</sup>Donald G. Fleming, Randall J. Mikula, and David M. Garner, *J. Chem. Phys.* **73**, 2751 (1980).

<sup>12</sup>C. J. Oram, J. B. Warren, G. M. Marshall, and J. Doornbos, *Nucl. Instrum. Methods* **179**, 95 (1981).

<sup>13</sup>A. E. Pifer, T. Bowen, and K. R. Kendall, *Nucl. Instrum. Methods* **135**, 39 (1976).

<sup>14</sup>R. L. Bunting and J. J. Kraushaar, *Nucl. Instrum. Methods* **118**, 565 (1974).

<sup>15</sup>R. F. Kiefl, J. B. Warren, G. M. Marshall, C. J. Oram, J. H. Brewer, D. J. Judd, and L. D. Spires, in *Hyperfine Interactions*, edited by A. J. Freeman and R. B. Frankel (Academic, New York, 1979), Vol. 6, p. 185.

<sup>16</sup>W. Brandt and R. Paulin, *Phys. Rev. Lett.* **21**, 193 (1968).

<sup>17</sup>S. Chandrasekhar, *Rev. Mod. Phys.* **15**, 1 (1943).

<sup>18</sup>G. M. Marshall, Ph.D. thesis, University of British Columbia, 1981 (unpublished).

<sup>19</sup>R. J. Mikula, D. M. Garner, D. G. Fleming, G. M. Marshall, and J. H. Brewer, in *Hyperfine Interactions* (Ref. 15), Vol. 6, p. 379. See also B. A. Barnett, C. Y. Chang, C. B. Yodh, J. B. Carroll, M. Eckhause, C. S. Hsieh, J. R. Kane, and C. B. Spence, *Phys. Rev. A* **11**, 39 (1975).